

# Passive Models of Neurons in the Deep Cerebellar Nuclei: the Effect of Reconstruction Errors

Volker Steuber <sup>a,1</sup>, Erik De Schutter <sup>a</sup> and Dieter Jaeger <sup>b</sup>

<sup>a</sup>*Laboratory of Theoretical Neurobiology, Born-Bunge Foundation,  
University of Antwerp, B-2610 Antwerp, Belgium*

<sup>b</sup>*Department of Biology, Emory University, Atlanta, Georgia 30322, USA*

---

## Abstract

Whole cell patch-clamp recordings were made from deep cerebellar nucleus neurons in slices from 14-day old rats. Neurons were reconstructed independently by two persons and converted into detailed compartmental models. The specific capacitance  $C_M$ , membrane resistivity  $R_M$  and axial resistivity  $R_A$  were optimised for each reconstructed cell by fitting the model responses to electrophysiological data using a genetic algorithm. The differences between different reconstructions of the same cell led to variations of up to 19% in  $C_M$ ,  $R_M$  and  $R_A$ . Taking into account shrinkage and realistic errors in diameter measurements, even larger variations of up to 173% were found.

*Key words:* Deep Cerebellar Nuclei, Passive Neuron Model, Reconstruction, Genetic Algorithm.

---

## Summary

The deep cerebellar nuclei (DCN) provide the main output from the cerebellum to the rest of the brain. Three different types of DCN neurons have been described: large glutamatergic neurons which project to the thalamus, red nucleus and other brain stem nuclei, smaller GABAergic neurons which carry feedback signals to the inferior olive, and even smaller interneurons which colocalise both GABA and glycine [4,2,14]. In this study, whole cell patch-clamp

---

<sup>1</sup> Corresponding author, *e-mail address:* volker@bbf.uia.ac.be

**Poster Presentation preferred.**

recordings were made from somata of large DCN neurons in slices from 14-day old rats. Similar to previous observations [1,6,11,5], the neurons fired spontaneously and regularly at a frequency of  $15.5 \pm 9.8$  Hz ( $n = 15$ ). To construct a passive model, ion channels and synaptic inputs were blocked with TTX, TEA,  $\text{Cd}^{2+}$ ,  $\text{Cs}^+$ , 4-AP, CNQX and picrotoxin. The voltage responses to long (1s) current pulses were checked for linear scaling [10]. The neurons had an average input resistance of  $R_N = 452 \pm 165 M\Omega$  ( $n = 15$ ). If the neurons behaved passively, voltage responses to short current pulses were recorded ( $+0.5\text{nA}$  and  $-1\text{nA} \times 0.5\text{ms}$ ). The prepulse voltage baseline was subtracted, the traces were scaled by  $1/\text{current}$  and filtered with a time dependent Gaussian filter ( $\sigma = 0.05t$ ) [9]:

$$V_{new}(t) = \frac{1}{\sqrt{2\pi}\sigma} \int_{-\infty}^{+\infty} ds \exp(-s^2/2\sigma^2) V_{old}(t+s) \quad (1)$$

Very noise traces were rejected, the grand average of all voltage traces was calculated, and the time constant  $\tau_0 = R_M C_M$  was used to obtain an initial estimate of  $R_M$  for compartmentalisation (assuming a standard value of  $C_M = 1\mu\text{F}/\text{cm}^2$ ).

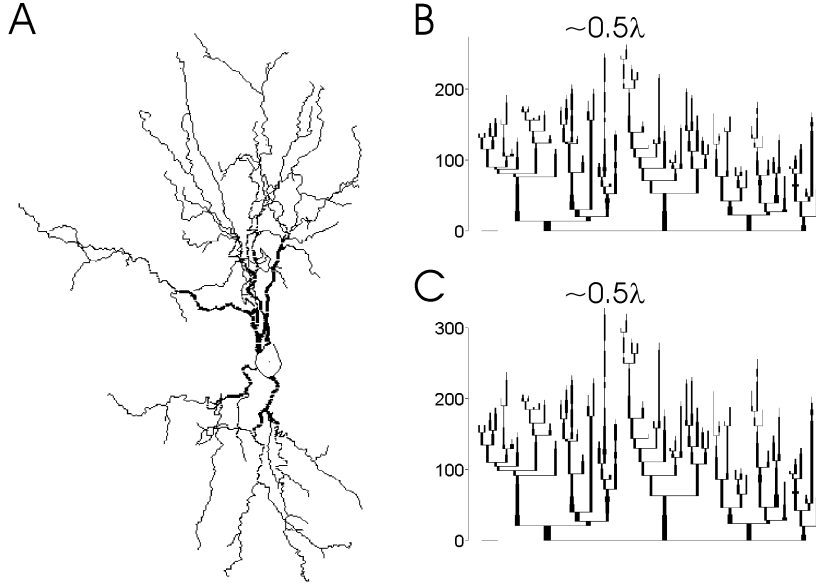


Fig. 1. Morphology (A) and dendrograms (B,C) of the large DCN cell cn0106c. B shows the original dendrogram, in C a shrinkage correction factor of 2 has been applied along the z-axis. The horizontal bars in B and C indicate  $10\mu\text{m}$ .

During the recordings, the neurons were filled with biocytin. After fixation, staining and mounting, two cells with a soma diameter  $\geq 20\mu\text{m}$  were reconstructed using the Neurolucida system (the morphology of one of the cells is shown in Fig. 1A). Neither of the cells had any spines, but a few filiform appendages were found that were included in the reconstruction [14].

One of these cells, *cn0106c*, was reconstructed independently by two persons. The CVAPP software (Robert Cannon, see [www.compneuro.org](http://www.compneuro.org)) was used to convert the Neurolucida files into cell parameter files for the neural simulator GENESIS [3]. The voltage responses of the reconstructed cells to short current pulses were simulated in GENESIS. Using a genetic algorithm (GA) with uniform crossover, fitness ranking and a constant mutation probability of 0.1, the values of  $C_M$ ,  $R_M$  and  $R_A$  were optimised for each reconstructed cell by matching the simulated response with electrophysiological data from the same cell. The fitness criterion for the GA was the negative root mean square error (RMSE) of the model response compared with the experimental response, and a model was considered fit enough if the RMSE was  $\leq 1\%$  of the average voltage response. The GA constrained the parameters to the following ranges:  $0.5\mu F/cm^2 \leq C_M \leq 2.5\mu F/cm^2$ ,  $5k\Omega cm^2 \leq R_M \leq 200k\Omega cm^2$  and  $20\Omega cm \leq R_A \leq 300\Omega cm$ . Separate GAs were run assuming non-uniform specific membrane resistivities, but in no case did this result in an improvement of the final fit. Figs. 2 and 3 show the evolution of the parameter values, their fitness and the corresponding voltage traces for one of the reconstructions of cell *cn0106c*.

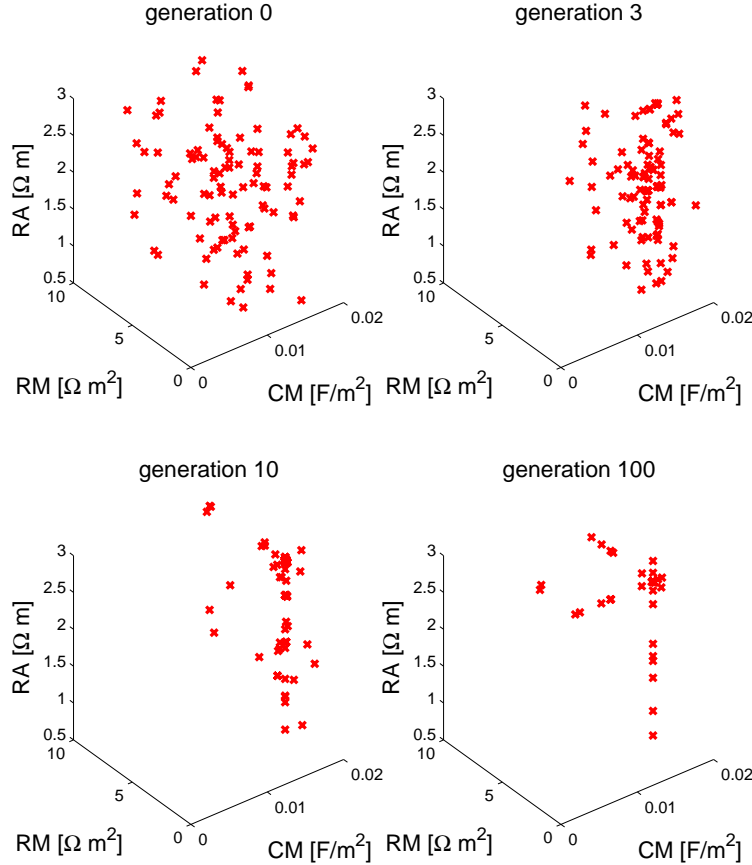


Fig. 2. Evolution of 100 sets of values for  $C_M$ ,  $R_M$  and  $R_A$  during the GA based fitting of the first reconstruction of *cn0106c*.

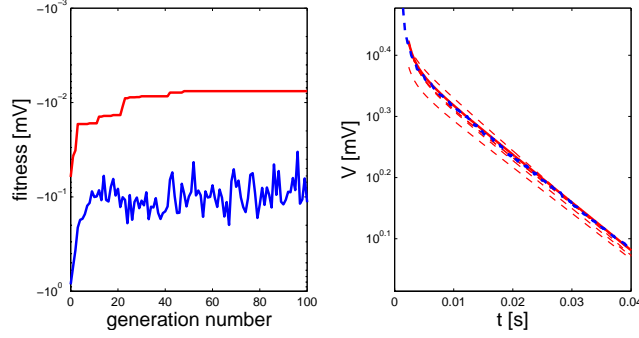


Fig. 3. Left: evolution of maximum (red) and average (blue) fitness during the GA based fitting of the first reconstruction of *cn0106c*. Right: experimentally recorded voltage response (blue) and evolution of the model responses (dashed red) during the fitting. The final fit is shown in solid red.

The final values for the first reconstruction of *cn0106c* were  $C_M = 1.70 \mu F/cm^2$ ,  $R_M = 32.7 k\Omega cm^2$  and  $R_A = 262 \Omega cm$ . As it is very easy to introduce errors in dendritic diameters [8], the cell was reconstructed by somebody else and the fitting repeated, resulting in  $C_M = 1.43 \mu F/cm^2$ ,  $R_M = 38.8 k\Omega cm^2$  and  $R_A = 300 \Omega cm$ . A second cell which was reconstructed had passive parameters in a similar range ( $C_M = 1.63 \mu F/cm^2$ ,  $R_M = 34.4 k\Omega cm^2$  and  $R_A = 299 \Omega cm$ ).

The relative differences of  $C_M$ ,  $R_M$  and  $R_A$  between the two reconstructions of *cn0106c* were 19%, 19% and 14.5%, respectively. Because of these large differences, we decided to study the effect of diameter errors on passive cable parameters more systematically. The largest and smallest dendritic diameters in the first reconstruction were  $3.84 \mu m$  and  $0.35 \mu m$ , compared to  $4.47 \mu m$  and  $0.23 \mu m$  in the second reconstruction. This corresponds to a relative difference of 16% and 52% for the largest and smallest dendrite, respectively. To reproduce the larger relative error for smaller dendrites, we ran GA based fits for a range of cell parameter files that had been generated by changing all dendritic diameters to:

$$d_{new} = d_{old} + f_d \frac{d_{old}}{d_{old} + k} \quad (2)$$

where  $k = 2 \mu m$ ,  $-1 \leq f_d \leq 1$  is the diameter correction factor and  $d_{old}$  are the dendritic diameters in the first reconstruction of *cn0106c*. For  $f_d = 1$ , this introduced a maximum diameter error of  $0.67 \mu m$  for  $d = 4 \mu m$  dendrites and  $0.11 \mu m$  for  $d = 0.25 \mu m$  dendrites, both of which are in a realistic range. Varying dendritic diameters in this way resulted in passive parameter values in the range between  $C_M = 1.32 \mu F/cm^2$ ,  $R_M = 41.2 k\Omega cm^2$ ,  $R_A = 300 \Omega cm$  (for  $f_d = 1$ , i.e. thick dendrites) and  $C_M = 2.37 \mu F/cm^2$ ,  $R_M = 23.6 k\Omega cm^2$ ,  $R_A = 142 \Omega cm$  (for  $f_d = -1$ , i.e. thin dendrites). Thus, realistic errors in dendritic diameters can introduce errors of up to 111% in passive cable parameters. The same results were obtained in a set of simulations where the dendritic diameter change factor  $f_d$  was made an additional parameter optimised by the GA.

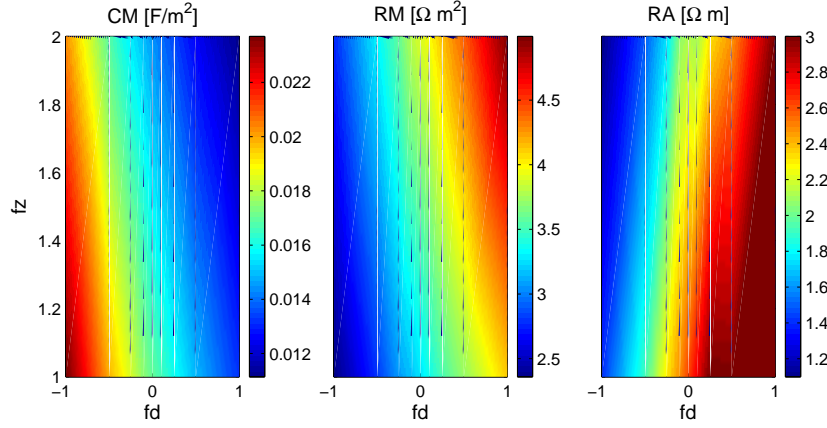


Fig. 4. Range of values of  $C_M$ ,  $R_M$  and  $R_A$  for different diameter change factors  $f_d$  and z-axis correction factors  $f_z$  that have been applied to the reconstruction of *cn0106c*.

Another factor that can have a significant impact on passive parameters is tissue shrinkage during fixation and mounting of slices. Although the shrinkage in x and y direction is usually neglectable [7,13,14], shrinkage by factors of 3.7 and 2.8 in z direction has recently been reported in morphological studies of DCN neurons [14] and cortical pyramidal cells [7]. In our preparation, the thickness of slices after coverslipping was found to be reduced by factors of up to 2. We studied the effect of shrinkage by applying correction factors  $f_z$  between 1 and 2 along the z-axis of our first reconstruction of *cn0106c*. A z-axis correction of  $f_z = 2$  resulted in values of  $C_M = 1.44 \mu F/cm^2$ ,  $R_M = 39.1 k\Omega cm^2$  and  $R_A = 213 \Omega cm$ . Dendrograms of the original reconstruction of *cn0106c* and the shrinkage corrected version with  $f_z = 2$  are shown in Fig. 1 B and C. In both cases, the electrotonic length of the longest dendrite is approximately  $0.5\lambda$ , indicating an electrically compact cell.

Although a large range of passive cable parameter values can be found in the literature [12,9], values of the z-axis corrected reconstruction were closer to more recently published numbers [13]. The combination of shrinkage and diameter errors could lead to values for  $C_M$  between  $1.11$  and  $2.37 \mu F/cm^2$ ,  $R_M = 23.6 - 49.9 k\Omega cm^2$  and  $R_A = 110 - 300 \Omega cm$  (Fig. 4). Thus, faulty shrinkage correction and diameter measurement errors can introduce errors of up to 173% in the passive cable parameters.

## Acknowledgements

Many thanks to Tibor Szilagyi for helpful discussions and for providing his neuronal morphology analysis program and to Svetlana Gurvich for help with the reconstructions. The work was supported by the NIMH grant MH57256, the FWO (Flanders) and a Human Frontier Science Program Organization long-term fellowship to VS.

## References

- [1] C. D. Aizenman and D. J. Linden, Regulation of the rebound depolarization and spontaneous firing patterns of deep nuclear neurons in slices of rat cerebellum, *J. Neurophysiol.* 82 (1999) 1697-1709.
- [2] C. Batini, C. Compoint, C. Buisseret-Delmas, H. Daniel and M. Guegan, Cerebellar nuclei and the nucleocortical projections in the rat: retrograde tracing coupled to GABA and glutamate immunohistochemistry, *J. Comp. Neurol.* 315 (1992) 74-84.
- [3] J. M. Bower and D. Beeman, *The Book of GENESIS: Exploring Realistic Neural Models with the GEneral NEural SIMulation System* (Telos, Springer Verlag, New York, second edition, 1998).
- [4] V. Chan-Palay, *Cerebellar Dentate Nucleus: Organization, Cytology and Transmitters* (Springer Verlag, Berlin, 1977).
- [5] U. Czubyko, F. Sultan, P. Thier and C. Schwarz, Two types of neurons in the rat cerebellar nuclei as distinguished by membrane potentials and intracellular fillings, *J. Neurophysiol.* 85 (2001) 2017-2029.
- [6] V. Gauck and D. Jaeger, The control of rate and timing of spikes in the deep cerebellar nuclei by inhibition, *J. Neurosci.* 82 (2000) 3006-3016.
- [7] B. Hellwig, A quantitative analysis of the local connectivity between pyramidal neurons in layers 2/3 of the rat visual cortex, *Biol. Cybern.* 82 (2000) 111-121.
- [8] D. Jaeger, Accurate reconstruction of neuronal morphology, in: E. De Schutter, ed., *Computational Neuroscience: Realistic Modeling for Experimentalists* (CRC Press, Boca Raton, 2000) 159-178.
- [9] G. Major, A. U. Larkman, P. Jonas, B. Sakmann and J. Jack, Detailed passive cable models of whole-cell recorded CA3 pyramidal neurons in rat hippocampal slices, *J. Neurosci.* 14 (1994) 4613-4638.
- [10] G. Major, Passive cable modeling - a practical introduction, in: E. De Schutter, ed., *Computational Neuroscience: Realistic Modeling for Experimentalists* (CRC Press, Boca Raton, 2000) 209-232.
- [11] I. M. Raman, A. E. Gustafson and D. Padgett, Ionic currents and spontaneous firing in neurons isolated from the cerebellar nuclei, *J. Neurosci.* 20 (2000) 9004-9016.
- [12] M. Rapp, I. Segev and Y. Yarom, Physiology, morphology and detailed passive models of guinea-pig cerebellar Purkinje cells, *J. Physiol.* 474 (1994) 101-118.

- [13] A. Roth and M. Hausser, Compartmental models of rat cerebellar Purkinje cells based on simultaneous somatic and dendritic patch-clamp recordings, *J. Physiol.* 535 (2001) 445-472.
- [14] F. Sultan, U. Czubayko and P. Thier, Morphological classification of the rat lateral cerebellar nuclear neurons by principal component analysis, *J. Comp. Neurol.* 455 (2003) 139-155.